Electronic Supplementary Material (ESI) for Journal of Materials Chemistry C.
This journal is © The Royal Society of Chemistry 2016

Supporting Information

Redox Tunable Viologen-based Porous Organic Polymers

Carol Hua, Bun Chan, Aditya Rawal, Floriana Tuna, David Collison, James M. Hook

*and Deanna M. D'Alessandro**

SYNTHESIS OF MONOMERS

Tris(p-ethynylphenyl)amine

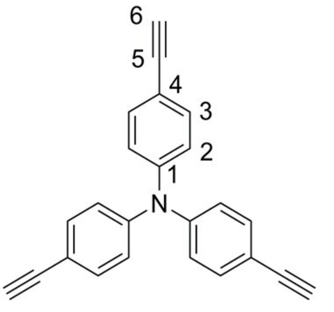

Tris(*p*-iodophenyl)amine (6.00 g, 9.65 mmol), $Pd(PPh_3)_2Cl_2$ (406 mg, 6 mol%, 0.579 mmol) and triphenylphosphine (75.9 mg, 3 mol%, 0.289 mmol) were added to dry and degassed triethylamine (100 mL). Ethynyltrimethylsilane (6.18 mL, 43.4 mmol) was added dropwise and the reaction mixture stirred for five minutes prior to the addition of copper iodide (55.0 mg, 0.289 mmol). The reaction mixture was stirred under nitrogen at room temperature for 24 hours, where a color change from yellow to green/brown was observed. The solvent removed under vacuum and the residue dissolved in diethyl ether and filtered through celite. The solvent was removed under vacuum from the filtrate to yield a light brown solid. The crude product was used in the next step without further purification.

If desired, the crude intermediate can purified by column chromatography (hexane gradient to 1:9 diethyl ether:hexane) to yield a light yellow solid.

^{1}H NMR (300 MHz, $CDCl_3$): 7.34 (d, ^3J(H2-H3) = 8.5 Hz, 6H; H2), 6.96 (d, ^3J(H2-H3) = 8.5 Hz, 6H; H3), 0.24 (s, 9H; CH_3 of TMS) ppm.

The crude tris(4-((trimethylsilyl)ethynyl)phenyl)amine (5.15 g) was suspended in methanol (90 mL) and potassium carbonate (4.27 g, 30.9 mmol) added. The reaction mixture was stirred at room temperature under nitrogen for 26 hours upon which the light brown suspension was observed to darken. The solvent was removed under vacuum to yield a brown sludge that was dissolved in ether and filtered. The filtrate was washed with water, dried over Na_2SO_4 and the solvent removed under vacuum. The crude product was purified by column chromatography (gradient hexane to 1:19 EtOAc:hexane to 1:9 EtOAc:hexane) to yield the product as a bright yellow solid (2.10 g, 67%).

^{1}H NMR (500 MHz, $CDCl_3$): 7.36 (d, ^3J(H2-H3) = 8.5 Hz, 6H; H2), 6.99 (d, ^3J(H2-H3) = 8.5 Hz, 6H; H3), 3.04 (s, 3H; CH of alkyne) ppm.

^{13}C{^{1}H} NMR (125 MHz, $CDCl_3$): 147.2 (C_q, C1), 133.5(CH, C2), 124.1 (CH, C3), 117.0 (C_q, C4), 83.5 (C_q, C5), 77.2 (C_q, C6) ppm.

1,1'-Bis(2,4-dinitrophenyl)-4,4'-bipyridine-1,1'-dium chloride

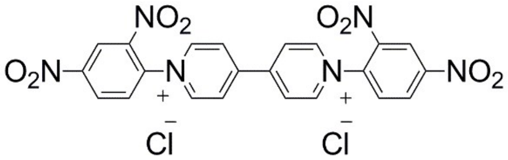

4,4'-Bipyridine (1.00 g, 6.40 mmol) was dissolved in ethanol (3 mL) and 2,4-dinitrochlorobenzene (3.63 g, 17.9 mmol) slowly added. Water (3 mL) was then added and the reaction mixture heated to 110 °C overnight, upon which the reaction mixture changed from a yellow suspension to a brown solution. The solvent was removed under vacuum and the residue redissolved in acetonitrile and filtered. The dark brown solid was washed with acetonitrile and diethyl ether to yield the product as a yellow solid that was dried under vacuum (2.50 g, 70%).

^{1}H NMR (200 MHz, MeOD): 9.72 (d, ^3J(H-H) = 5.8 Hz, 4H; CH), 9.38 (s, 2H; CH), 9.15 (d, ^3J(H-H) = 5.8 Hz, 4H; CH), 9.02 (d, ^3J(H-H) = 9.2 Hz, 2H; CH), 8.47 (d, ^3J(H-H) = 9.2 Hz, 2H; CH) ppm.

1,1’-bis(4-bromophenyl)-4,4’-bipyridinium chloride

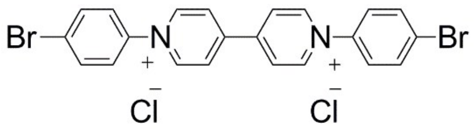

1,1’-Bis(2,4-dinitrophenyl)-4,4’-bipyridine-1,1’-diium chloride (0.500 g, 0.891 mmol) and 4-bromoaniline (306 μL, 2.67 mmol) were suspended in ethanol and heated at reflux under nitrogen for 22 hours resulting in the formation of a cloudy dark yellow reaction mixture. The solvent volume was reduced by evaporation and dropped into rapidly stirring THF to yield a fine yellow precipitate. This was filtered and the solid washed with ether to yield the product as a yellow solid (360 mg, 75%).

^{1}H NMR (300 MHz, D_2O): 9.44 (d, $^3J_{H\text{-}H}$ = 6.3 Hz, 4H; CH), 8.82 (d, $^3J_{H\text{-}H}$ = 6.3 Hz, 4H; CH), 7.99 (d, $^3J_{H\text{-}H}$ = 8.7 Hz, 4H; CH), 7.79 (d, $^3J_{H\text{-}H}$ = 8.7 Hz, 4H; CH) ppm.

A second crop was obtained by removing the solvent from the filtrate, dissolving in the minimum amount of ethanol and adding this solution to rapidly stirring THF dropwise.

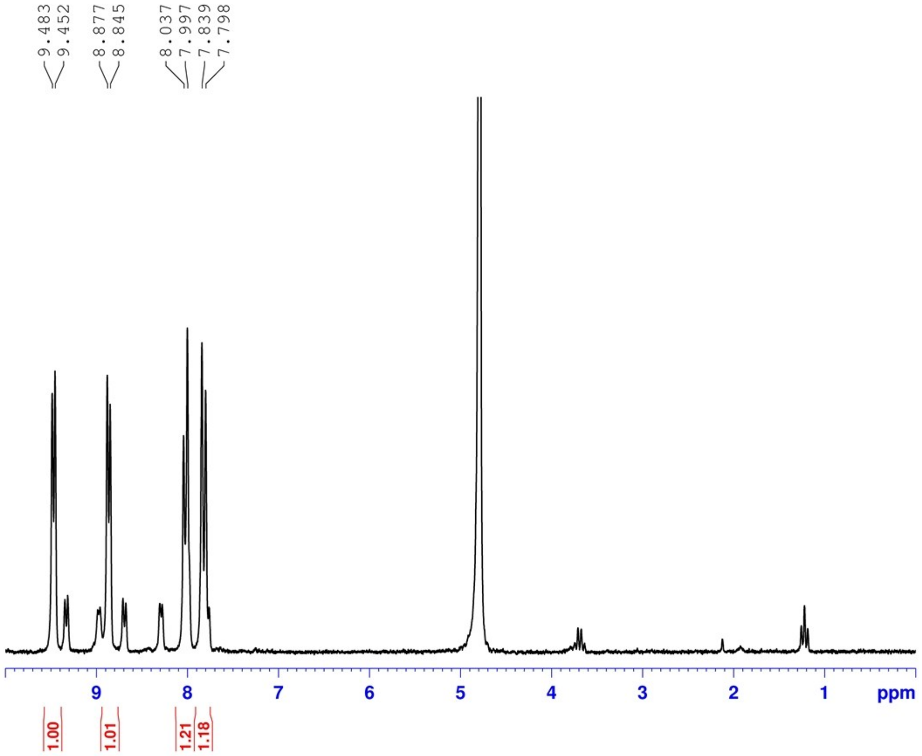

^{1}H NMR spectrum of 1,1’-bis(4-bromophenyl)-4,4’-bipyridinium chloride acquired in D_2O at 200 MHz.

FIGURES

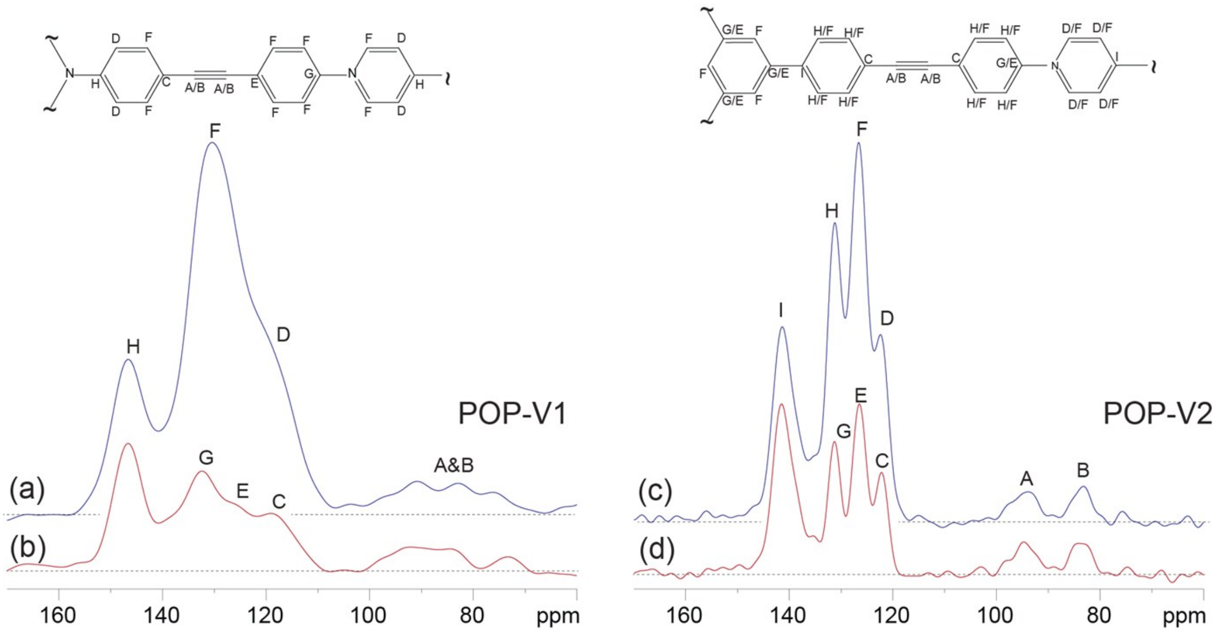

Figure S1. Solid state ^{13}C CPMAS NMR of a-b) POP-V1 and c-d) POP-V2. Spectra (b) and (d) are acquired after 40 µs of non-quaternary suppression, to enable assignment of the non-protonated carbon species. The spectra were acquired at 8 kHz MAS. The alphabetically labelled NMR peaks are assigned to the unique carbon sites in the structures of POP-V1 and POP-V2 as shown in the insets on top of the spectra. The uncertainty in the assignments of some of the peaks to a particular site are reflected in the insets.

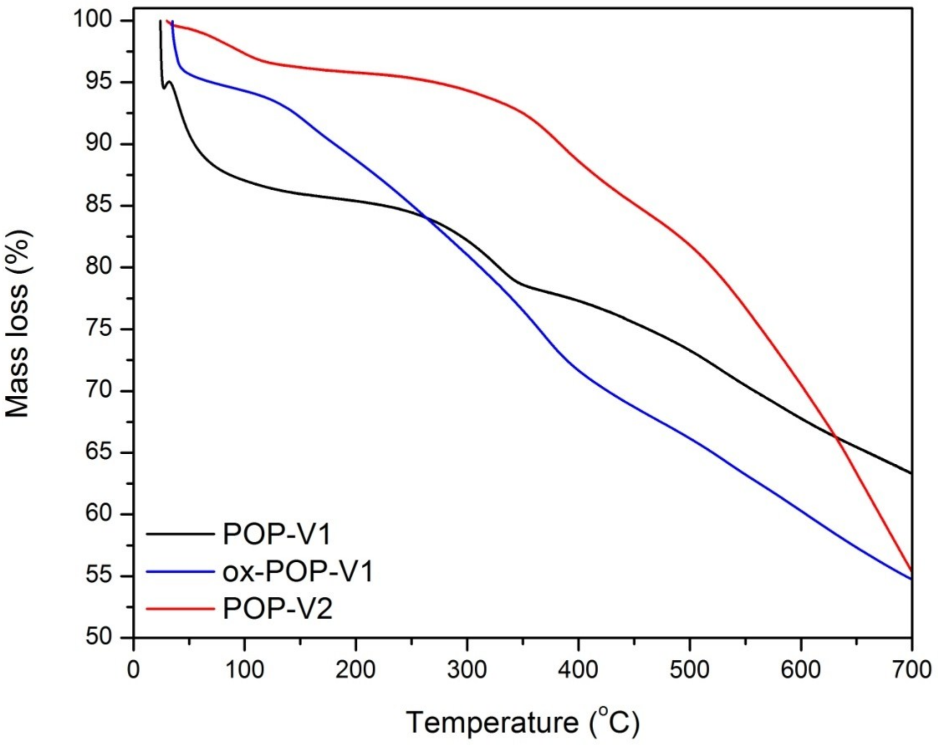

Figure S2. TGA of POP-V1, ox-POP-V1 and POP-V2 over the temperature range 25-700 °C.

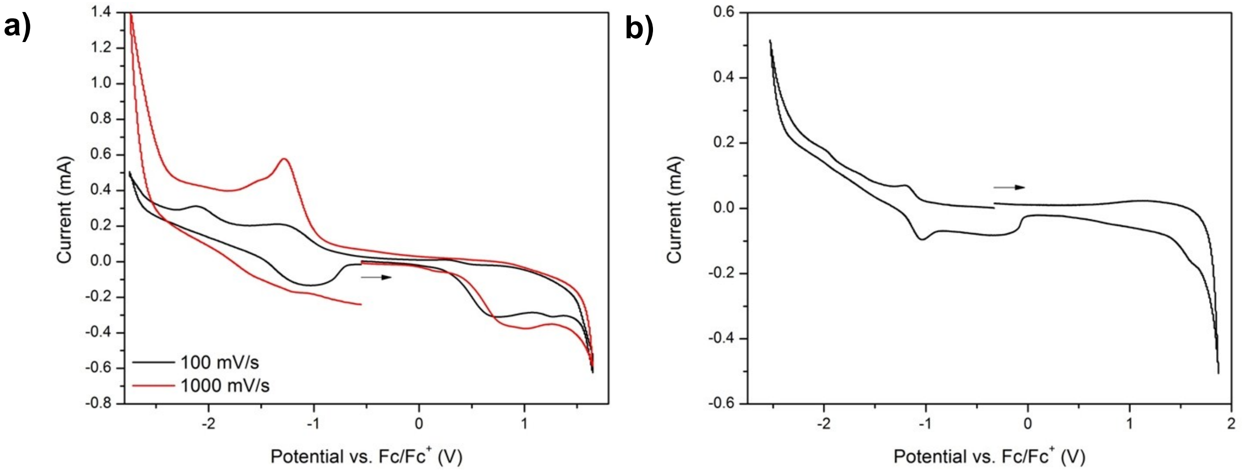

Figure S3. Electrochemistry of a) **POP-V1** and b) **POP-V2** in $[(n\text{-}C_4H_9)_4N]PF_6/CH_3CN$ at scan rates of 100 mV/s and 1000 mV/s, where the arrow indicates the direction of the forward scan.

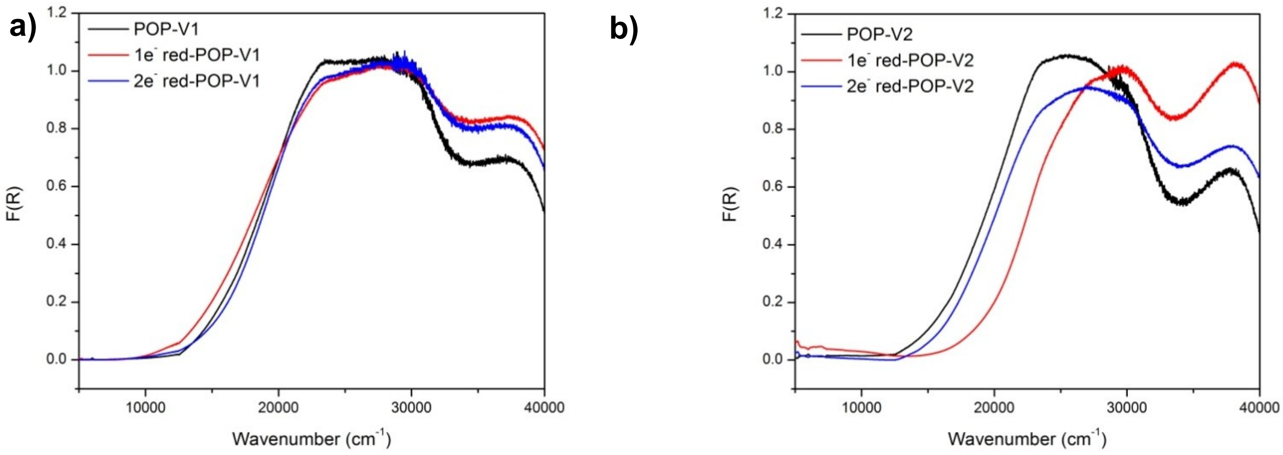

Figure S4. The solid state UV/Vis/NIR spectra of the neutral, 1 electron and 2 electron reduction of a) POP-V1 and b) POP-V2 over the range 5000-40000 cm^{-1}.

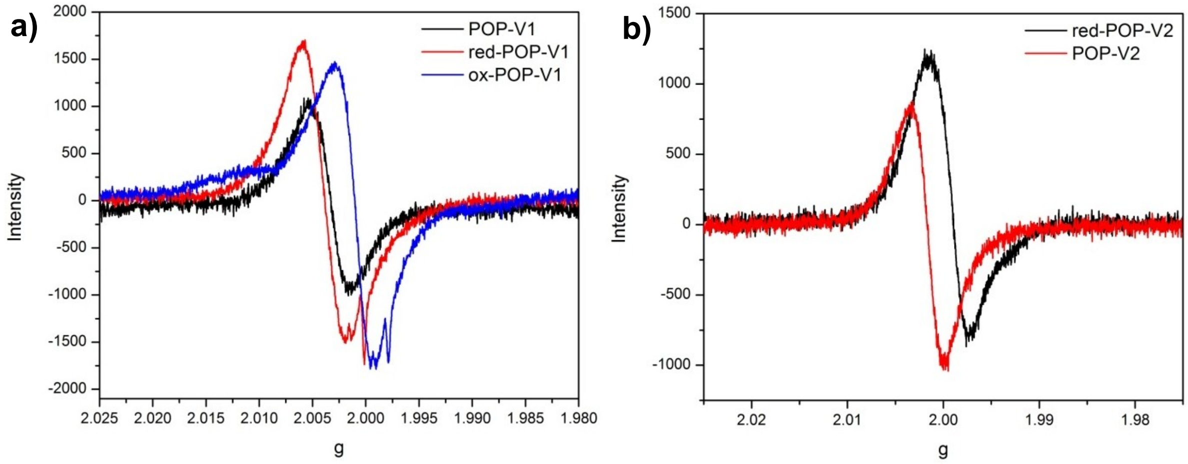

Figure S5. Solid state EPR spectra of a) POP-V1, ox-POP-V1 and red-POP-V1, b) POP-V2 and red-POP-V2 at X-Band at room temperature.

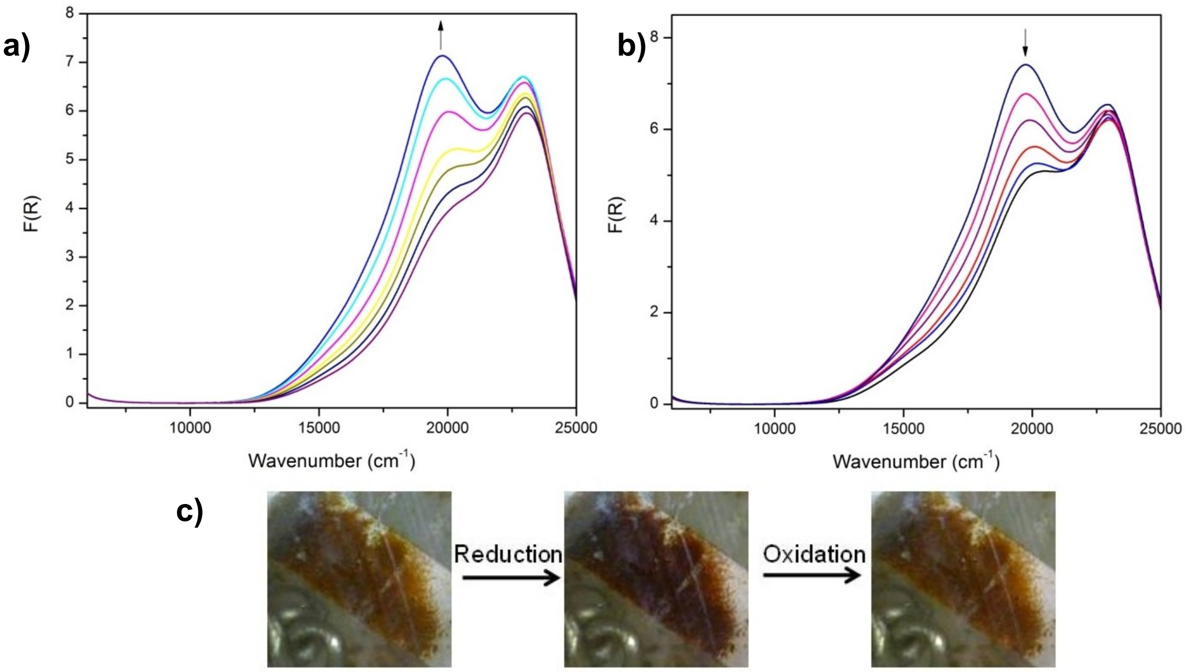

Figure S6. Solid state *in situ* spectroelectrochemical experiment in $[(n\text{-}C_4H_9)_4N]PF_6/CH_3CN$ for POP-V2 where a) oxidation (0 to 1.75 V), b) reduction (0 to -2.0 V) and c) photos of the oxidation/reduction.

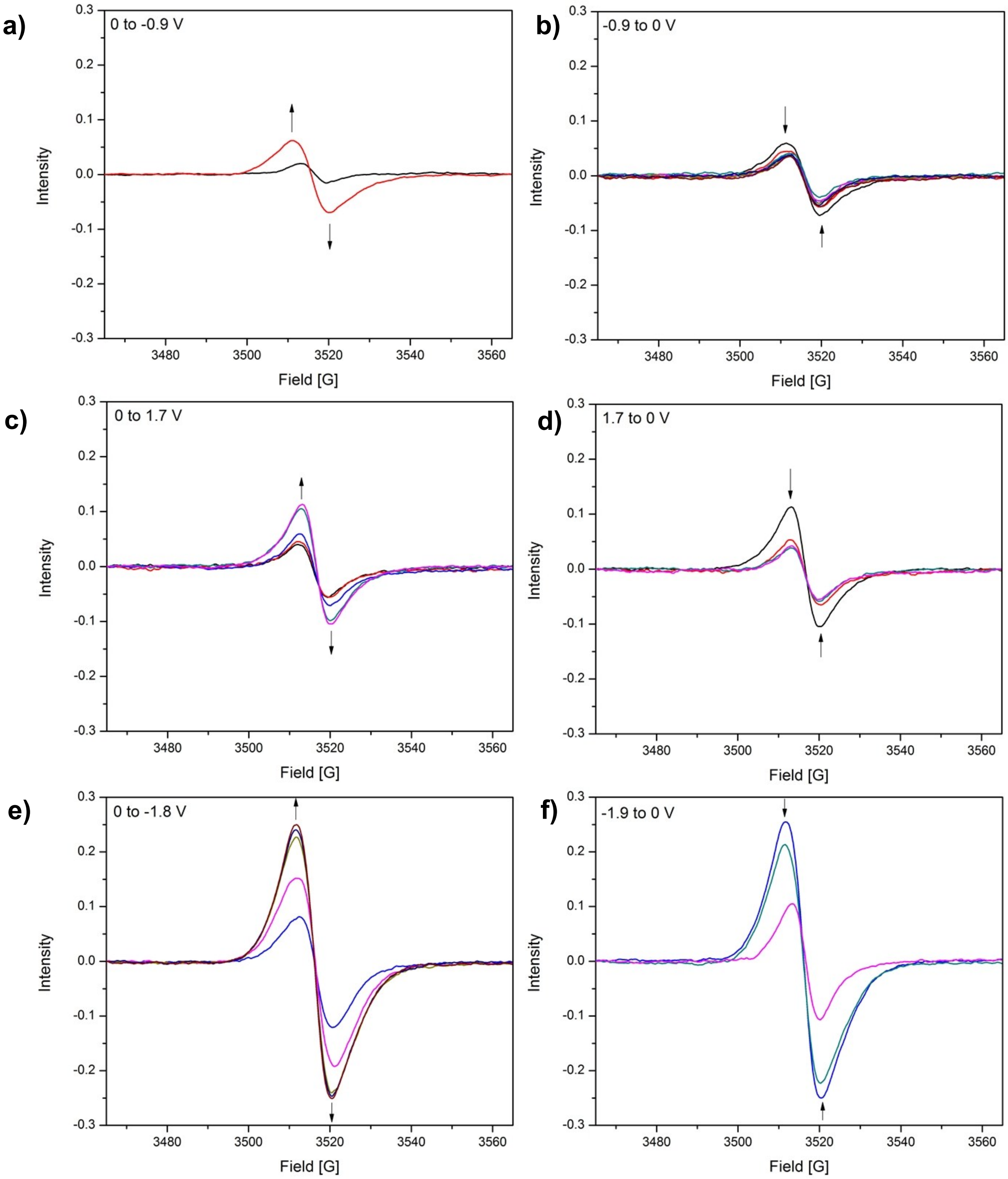

Figure S7. Solid state EPR spectroelectrochemical data for POP-V1 in $[(n\text{-}C_4H_9)_4N]PF_6/CH_3CN$ electrolyte where the signal intensity changed as a function of the applied potential. The sample was a) reduced to the radical cation of the viologen moiety (0 to -0.9 V), b) oxidized to the neutral form (-0.9 to 0 V), c) further oxidized to the radical cation of the triarylamine (0 to 1.7 V) then d) reduced to the neutral state (1.7 to 0 V), e) further reduced to the radical cation of the viologen (0 to -1.8 V) before f) being oxidized to the neutral state (-1.9 to 0 V).

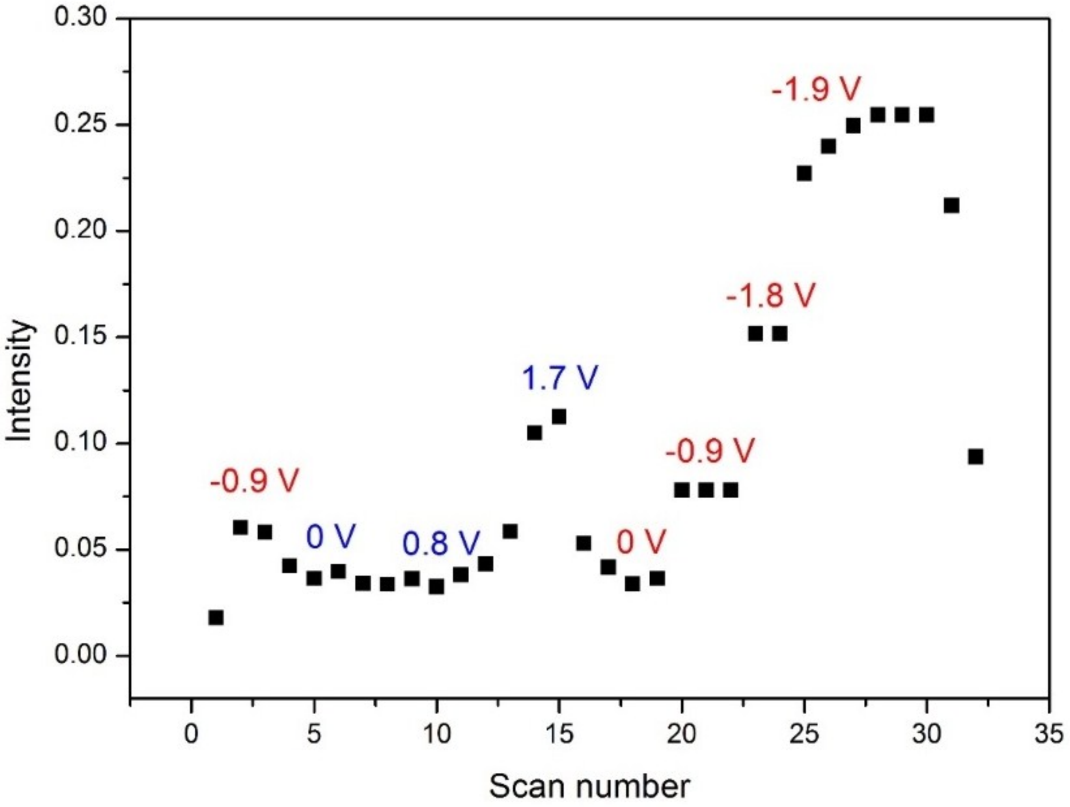

Figure S8. A plot of the signal intensity at 3511 G vs. scan number for POP-V1. The applied potentials are shown in the plot, where reductive potentials are in red and oxidative potentials in blue.

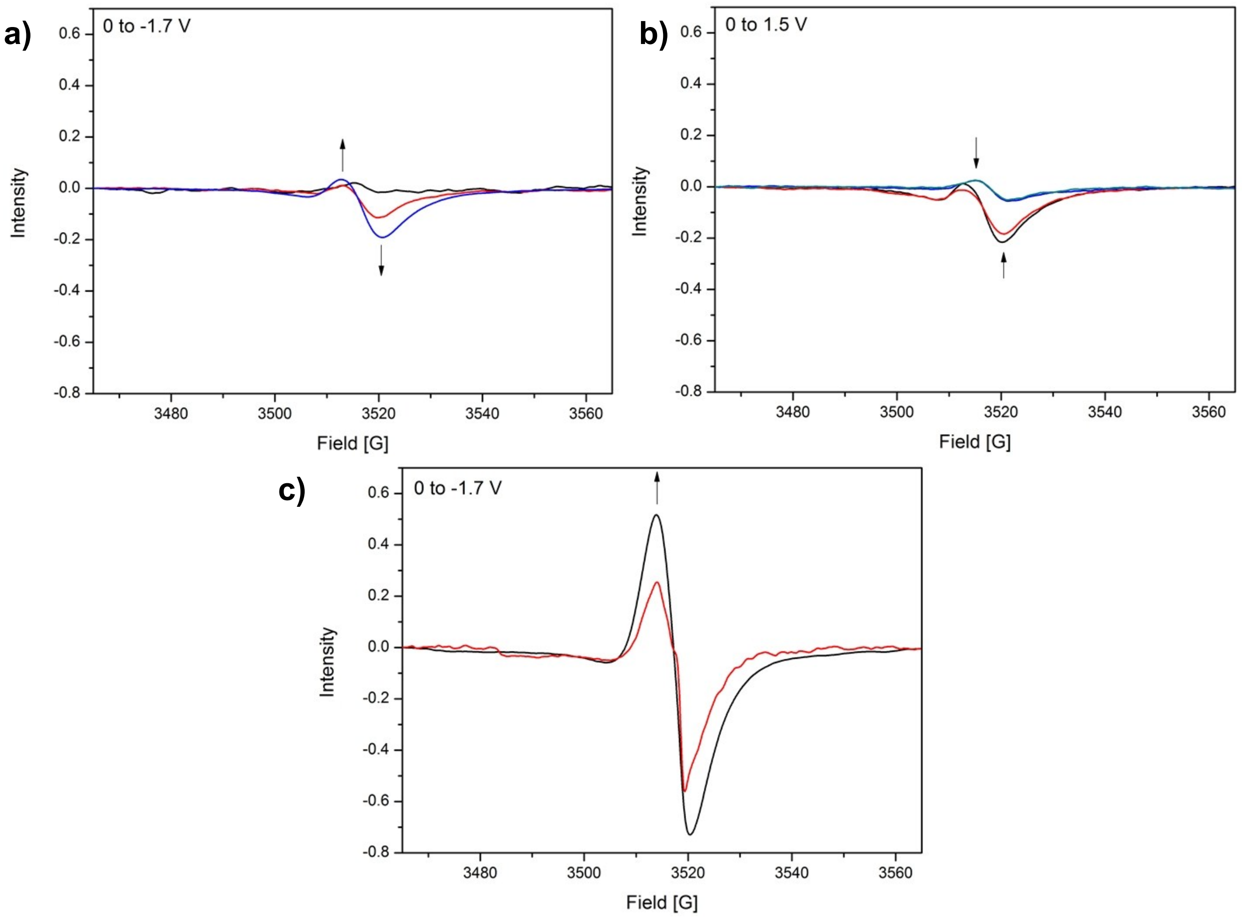

Figure S9. Solid state EPR spectroelectrochemical spectra of POP-V2 in [(n-C_4H_9)$_4$N]PF_6/CH_3CN electrolyte where the signal intensity changed as a function of the applied potential. The sample was a) reduced to form the viologen radical cation (0 to -1.7 V), b) oxidized to the neutral species (0 to 1.5 V) then c) reduced to reform the viologen radical cation (0 to -1.7 V).

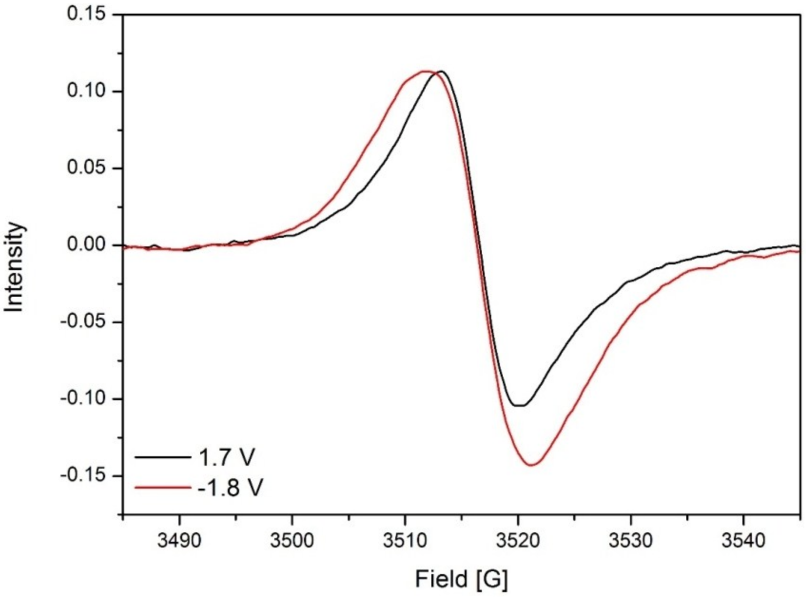

Figure S10. Spectroelectrochemical-EPR spectra of POP-V1 with an applied potential of 1.7 and -1.8 V in $[(n\text{-}C_4H_9)_4N]PF_6/CH_3CN$ electrolyte.

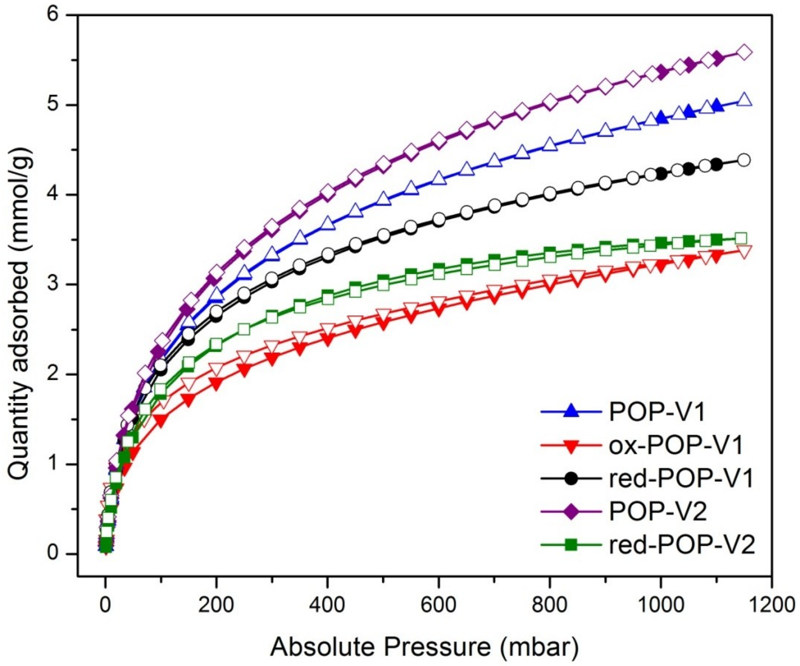

Figure S12. Gas sorption isotherms of POP-V1, ox-POP-V1, red-POP-V1 and POP-V2, red-POP-V2 for H_2 at 77 K where adsorption = filled symbols and desorption = open symbols. The lines joining each point are provided as a guide to the reader.

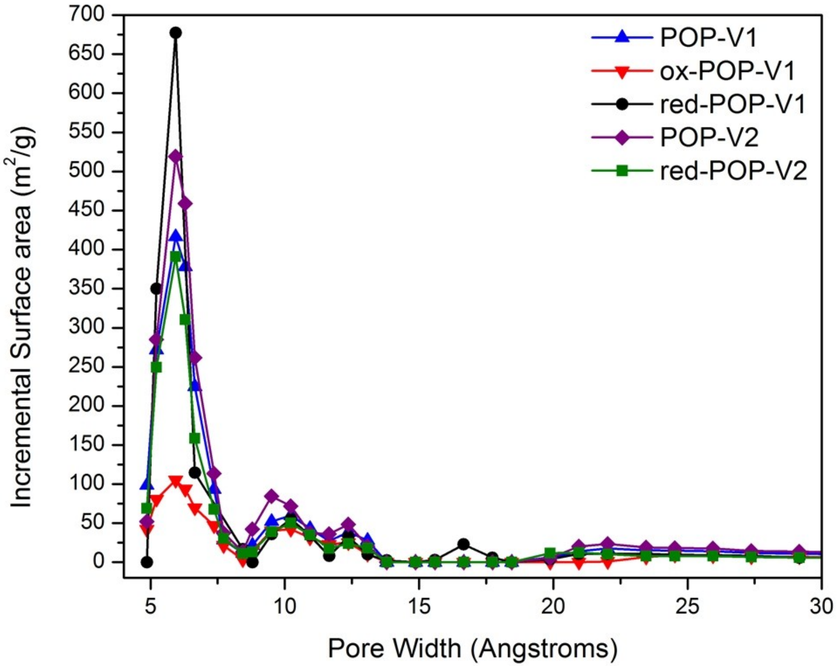

Figure S13. Pore size analysis of POP-V1, red-POP-V1, ox-POP-V1, POP-V2 and red-POP-V2. The lines joining each point are provided as a guide to the reader.

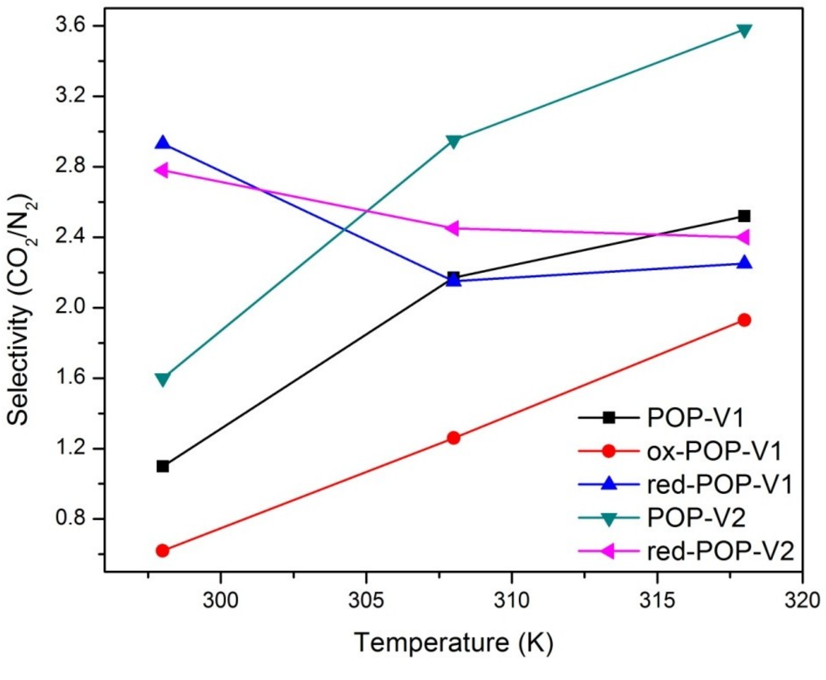

Figure S13: Single point selectivity values for CO_2 (0.15 bar) over N_2 (0.75 bar) at 295, 305 and 315 K.

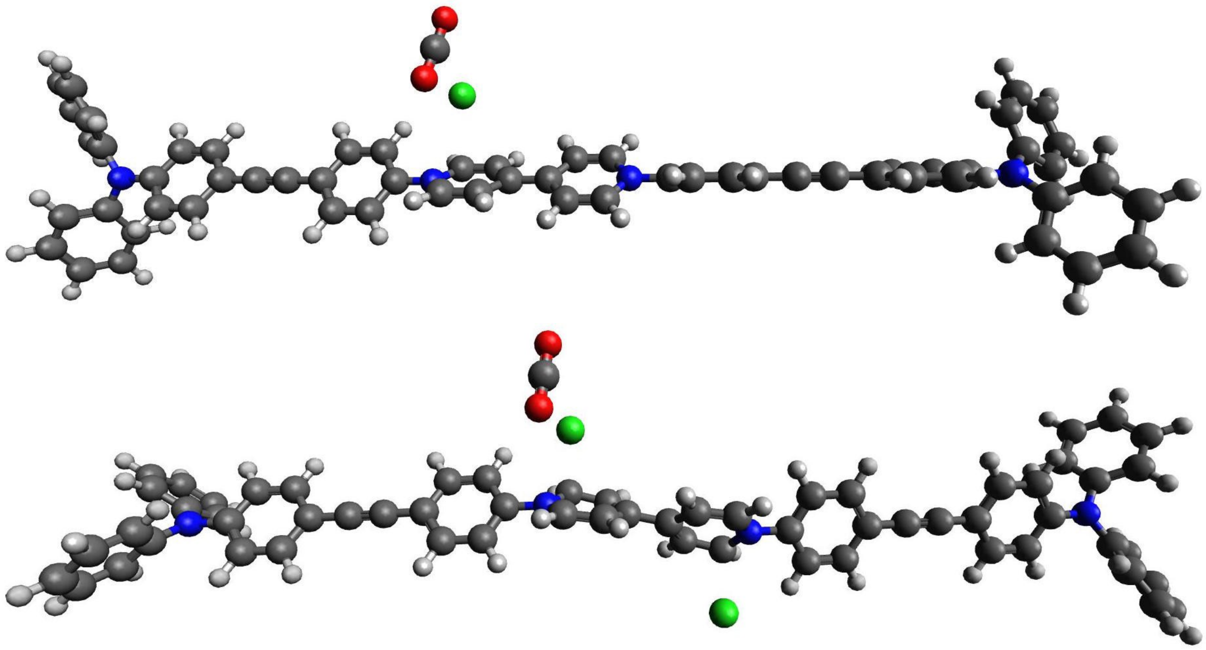

Figure S15. The structures of the monomer POP-V1 polymer fragments, mPOP-V1(Cl), and mPOP-V1(Cl)$_2$ with CO$_2$ where C = grey, N = blue, H = white, O = oxygen, Cl = green.